

Structural Studies on *N*-(1-naphthyl)-3-amino-5-oxo-4-phenyl-1*H*-pyrazole-1-carboxamide with Antibacterial Activity

Agnieszka A. Kaczor¹, Tomasz Wróbel¹, Zbigniew Karczmarzyk², Waldemar Wysocki², Andrzej Fruzinski³, Malgorzata Brodacka², Dariusz Matosiuk¹ and Monika Pitucha^{4*}

¹Department of Synthesis and Chemical Technology of Pharmaceutical Substances with Computer Modeling Lab, Faculty of Pharmacy with Division of Medical Analytics, Medical University of Lublin, 4A Chodźki St., PL-20093 Lublin, Poland and University of Eastern Finland, School of Pharmacy, Department of Pharmaceutical Chemistry, Yliopistonranta 1, P.O. Box 1627, FI-70211 Kuopio, Finland; ²Department of Chemistry, Siedlce University, 3 Maja 54 St., PL-08110 Siedlce, Poland; ³Institute of General and Ecological Chemistry, Technical University, Żeromskiego 115 St., PL- 90924 Łódź, Poland; ⁴Department of Organic Chemistry, Faculty of Pharmacy with Division of Medical Analytics, 4A Chodźki St., PL-20093 Lublin, Poland

Received March 24, 2013; Revised August 16, 2013; Accepted September 04, 2013

Abstract: The structure and tautomerism of *N*-(1-naphthyl)-3-amino-5-oxo-4-phenyl-1*H*-pyrazole-1-carboxamide with antibacterial activity have been investigated with experimental approaches (X-ray studies, IR, ¹H and ¹³C NMR spectra, including NOESY and N-HSQC spectra) and quantum chemical calculations. It is found that the tautomer with the keto group in position 5 is energetically privileged in the crystalline state while in DMSO and water solution the equilibrium is shifted towards the form with the hydroxyl group at this position. These findings are related to antibacterial activity of the studied compound and are crucial for future molecular docking and structure-activity relationship studies.

Keywords: Antibacterial compounds, pyrazolones, quantum chemical calculations, tautomerism, X-ray structure determination.

INTRODUCTION

Elucidation of structure of organic compounds with biological activity is crucial in order to rationalize their activity, to enable molecular docking studies, and for structure-activity relationship analysis. In particular, structural studies are important for compounds which can occur in different tautomeric forms. The tautomerism and energetic prevalence of a particular tautomer may determine biological activity of a compound by promoting or preventing the formation of hydrogen bonds with its molecular target. The best known example of the significance of tautomerism for biological activity includes nitrogen bases present in DNA in which the stabilization of one tautomer ensures the possibility of formation of hydrogen bonds which stabilize the double helix structure.

The tautomeric equilibrium between the keto and hydroxyl form occurs in many organic compounds, including heterocyclic compounds. Previously, we found that stabilization of one tautomer is important for the activity of 1-aryl-4,5-dihydro-1*H*-imidazol-2-amine derivatives towards opioid receptors [1-4], and for the anticancer activity of 4-benzyl-3-[(1-methylpyrrol-2-yl)methyl]-4,5-dihydro-1*H*-1,2,4-triazol-5-one, probably acting through EGFR tyrosine kinase [5].

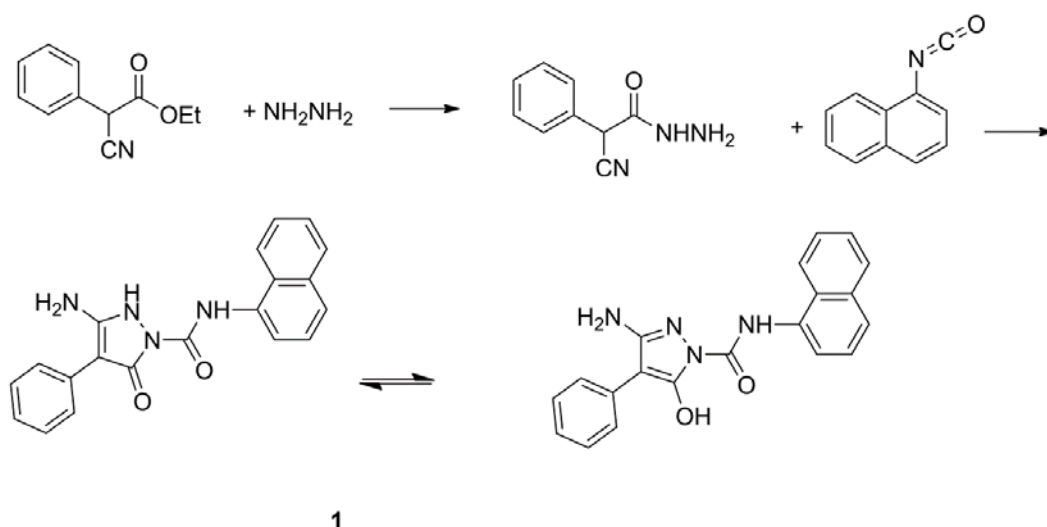
Recently, we have focused on compounds with pyrazole moiety. Pyrazole derivatives are known as herbicides, fungicides, insecticides, MDR modulators and also antibacterial, anti-inflammatory, anti-tumor, antihyperglycemic, antipyretic and analgesic agents [6-15]. Some compounds with the pyrazole moiety exhibit HIV-1 reverse transcriptase and IL-1 synthesis inhibitory activity [15]. Here we present the experimental (X-ray studies, IR, ¹H and ¹³C NMR spectra, including NOESY and N-HSQC spectra) and computational studies on the structure and tautomerism of *N*-(1-naphthyl)-3-amino-5-oxo-4-phenyl-1*H*-pyrazole-1-carboxamide. We find that although the keto tautomer is the one present in the crystalline state, in DMSO and water solutions the tautomeric equilibrium is shifted towards the tautomer with the hydroxyl group.

MATERIALS AND METHODS

Chemistry

N-(1-naphthyl)-3-amino-5-oxo-4-phenyl-1*H*-pyrazole-1-carboxamide was obtained as reported earlier: a mixture of 1.75g (0.01 moles) of 1-cyanophenylacetic acid hydrazide and 0.01 moles of 1-naphthyl isocyanate in 10 ml of acetonitrile was kept for 24 hours at room temperature [16]. Afterwards the compound formed was filtered off, washed with acetonitrile and crystallized from a methanol-acetonitrile (1:1) mixture (Scheme 1) [16].

*Address correspondence to this author at the Department of Organic Chemistry, Faculty of Pharmacy with Division of Medical Analytics, 4A Chodźki St., PL-20093 Lublin, Poland; Tel: 48-81-535-73-74; E-mail: monikapit@wp.pl



Scheme 1.

X-ray Structure Determination

X-ray data of **1** was collected on the Bruker SMART APEX II CCD diffractometer; crystal sizes 0.42x0.05x0.04 mm, CuK α ($\lambda = 1.54178$ Å) radiation, ω scans, $T = 100$ K, absorption correction: multi-scan SADABS [17], $T_{\min}/T_{\max} = 0.9281/1.0000$. The structure was solved by direct methods using SHELXS97 [18] and refined by full-matrix least-squares with SHELXL97 [18]. The N-bound H atoms were located by difference Fourier synthesis and refined freely. The remaining H atoms were positioned geometrically and treated as riding on their parent C atoms with C-H distances of 0.93 Å (aromatic). All H atoms were refined with isotropic displacement parameters taken as 1.5 times those of the respective parent atoms. All calculations were performed using WINGX version 1.64.05 package [19]. CCDC 929744 contains the supplementary crystallographic data for this paper. These data can be obtained free of charge at www.ccdc.cam.ac.uk/conts/retrieving.html [or from the Cambridge Crystallographic Data Centre (CCDC), 12 Union Road, Cambridge CB2 1EZ, UK; fax: +44(0) 1223 336 033; email: deposit@ccdc.cam.ac.uk].

Crystal data of 1: C₂₀H₁₆N₄O₂, $M = 344.373$, trigonal, space group $R\bar{3}$, $a = 35.3607(4)$, $c = 6.66720(10)$ Å, $V = 7219.64(16)$ Å³, $Z = 18$, $d_{\text{calc}} = 1.426$ Mg m⁻³, $F(000) = 3240$, $\mu(\text{Cu K}\alpha) = 0.775$ mm⁻¹, $T = 100\text{K}$, 3012 measured reflections (θ range 2.50–69.80°), 3012 unique reflections, final $R = 0.032$, $wR = 0.084$, $S = 0.907$ for 2928 reflections with $I > 2\sigma(I)$.

NMR Spectra

All NMR spectra were obtained on Bruker AVANCE III 600 MHz spectrometer with a BBO probe equipped with Z-gradient. Solvents were used as received from a commercial supplier. Tetramethylsilane was used as an internal standard for proton and carbon NMR spectra.

IR Spectra

IR spectra were recorded on a Thermo Nicolet 6700 FTIR spectrometer. Solids were measured utilizing the ATR

technique with the spectrometer equipped with a diamond Orbit stage. All solution measurements employed the transmittance technique using rigorously dried DMSO. The drying procedure was performed according to the standard method, i.e. standing over freshly activated alumina, filtering and distilling over CaH₂ under reduced pressure [20]. All manipulation with DMSO was conducted in Atmosbag filled with nitrogen to exclude any moisture coming from the air. The spectrum was run in a demountable cell (Pike Technologies) with KBr windows adjusted to 0.015 mm optical length. It consisted of 16 scans and spectral resolution of 4 cm⁻¹. First, the spectrum of the dried DMSO was recorded. Next, the spectrum of **1** in dried DMSO was taken and both spectra were overlapped for the correct assignments of the signals of **1** and subtraction of the DMSO signals.

Computational Details

The molecular structure of **1** in the ground state (*in vacuo*) was optimized with the B3LYP DFT (the variant of the DFT method using Becke's three parameter hybrid functional (B3) [21] with correlation functional such as the one proposed by Lee, Yang, and Parr (LYP) [22]) using 6-31G(d,p) as included in Gaussian09 [23]. Furthermore, Frontier Molecular Orbital (FMO) analysis was performed with Gaussian09 on the 6-31G(d,p)/B3LYP level of theory. The energy for both tautomers of **1** was calculated for isolated molecules (gas phase) and molecules in DMSO and water solutions. The population of both tautomeric forms was estimated using non-degenerate Boltzman distribution. 6-31G(d,p)/B3LYP calculations with Gaussian09 were also used to calculate the Continuous Set of Gauge Transformations (CSGT) [24-26] ¹H and ¹³C NMR chemical shifts as well as vibrational frequencies and infrared intensities. Calculations were performed using the Polarizable Continuum Model (PCM) [27]. This method creates a solute cavity *via* a set of overlapping spheres.

In the case of NMR chemical shifts DMSO was used as a solvent. The ¹H and ¹³C NMR chemical shifts were converted to the TMS scale by subtracting the calculated abso-

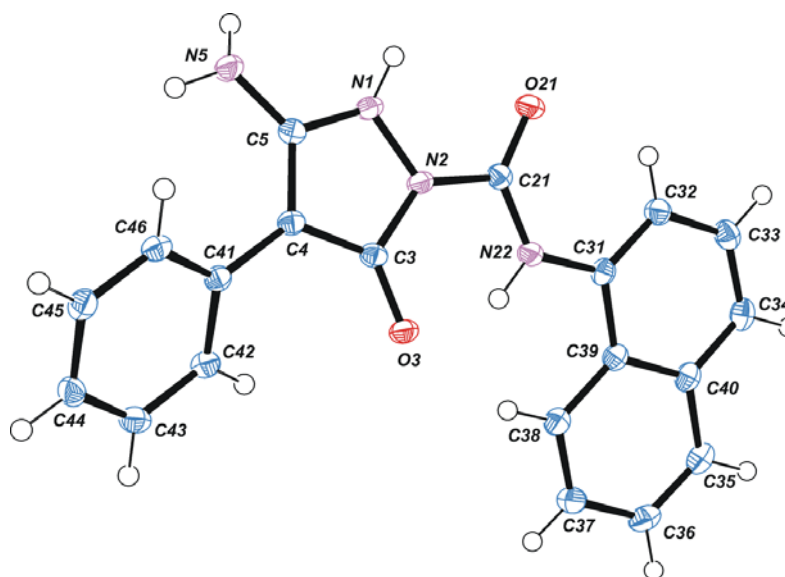


Fig. (1). A view of the X-ray molecular structure of **1** with the atomic labeling scheme (probability 50%).

Table 1. Hydrogen Bond Geometry of **1** (Å, °)

D-H...A	D-H	H...A	D...A	D-H...A
N22-H22...O3	0.914(19)	1.87(2)	2.6804(16)	146.2(15)
C32-H32...O21	0.93	2.30	2.9213(17)	123
C38-H38...N22	0.93	2.54	2.8509(17)	100
C42-H42...O3	0.93	2.56	3.082(2)	116
N1-H1...O21 ⁱ	0.862(19)	1.950(18)	2.7956(15)	167(2)
N5-H51...O3A ⁱⁱ	0.890(16)	2.030(18)	2.9050(13)	167.6(6)

(i) = 2/3-x, 1/3-y, 4/3-z; (ii) = x, y, 1+z

lute chemical shielding of TMS. These are 31.74 ppm and 190.92 ppm for 6-31G(d,p)/B3LYP for hydrogen and carbon atoms, respectively. The vibrational band assignments were made using ChemCraft [28], Pymol v. 0.99 [29], Discovery Studio v. 3.1 [30], Yasara Structure [31], Mercury [32] and ArgusLab [33] were also used for visualization of results.

RESULTS AND DISCUSSION

X-ray and Computed Structure of **1**

X-ray analysis of compound **1** was performed in order to confirm the synthesis pathway and identification of its tautomeric form in the solid state. The structure and conformation of the molecule **1** in the crystal are shown in (Fig. 1). In the crystalline state, the molecule exists in N22-amino/O21-keto tautomeric form, as evidenced by the C21-O21 bond length of 1.2195(13) typical for the carbonyl group and the positions of the H atom in the vicinity of N22 in the difference electron-density map. The geometry (bond lengths, angles and planarity) of the pyrazole-carboxamide system is very similar in **1** and the closely related structure of *N*-ethoxycarbonylmethyl-3-amino-5-hydroxy-4-phenyl-1*H*-pyrazole-1-carboxamide and *N*-butyl-3-amino-5-hydroxy-4-phenyl-1*H*-pyrazole-1-carboxamide [16]. In **1**, similarly

as in the above-mentioned structures, the carbonyl group of the carboxamide moiety adopts a *cis* conformation in respect to N-N bond in pyrazole ring with the torsion angle N1-N2-C2-O21 of 13.86(15)°. This conformation is stabilized by the intramolecular hydrogen bond N22-H22...O3 (Table 1). The torsion angles C3-C4-C4-C42 = -32.92(15)° and C21-N22-C31-C32 = 5.60(17)° show that the phenyl and naphthyl substituents have the *cis* conformation in respect to the pyrazole-carboxamide system forcing by the intramolecular C-H...X (X = O, N) interactions (Table 1).

In the crystal structure of **1** the intermolecular N1-H1...O21 hydrogen bond connects pairs of molecules into molecular dimers being in equi-positions (x, y, z) and (2/3-x, 1/3-y, 4/3-z) of the unit cell. These dimers form molecular chains parallel to *c* crystallographic axis *via* intermolecular N5-H51...O3 hydrogen bond (Table 1). Moreover, the π -electron systems of the pairs of pyrazole and benzene (C31...C40) rings belonging to the molecules at equi-positions (x, y, z) and (2/3-x, 1/3-y, 1/3-z) overlap each other, with centroid-to-centroid separation of 3.5674(9) Å and the angle between overlapping planes of 14.11(7)°.

The structure of **1** computed with the B3LYP DFT approach and 6-31G(d,p) basis set of Gaussian 09 was aligned

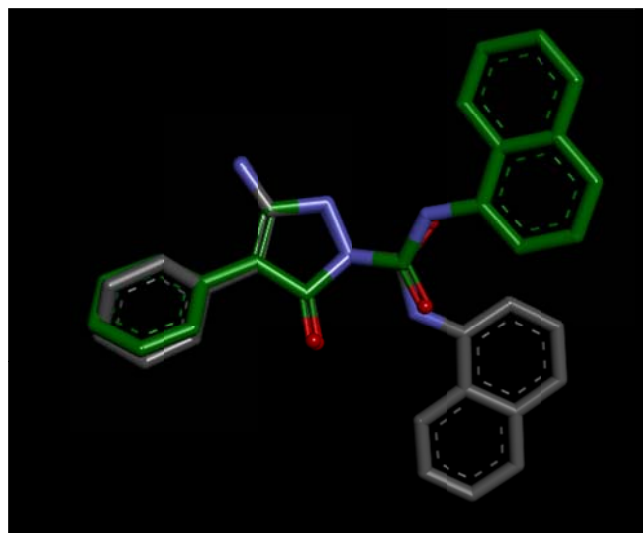


Fig. (2). Overlap of crystal and computed structures of **1** on the pyrazolone system. Hydrogen atoms not shown for clarity.

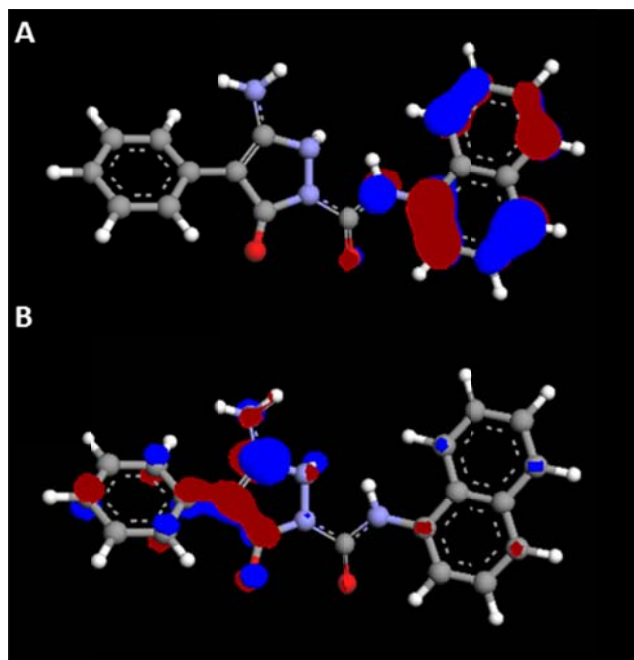


Fig. (3). HOMO (A) and LUMO (B) orbitals for the keto form of **1**.

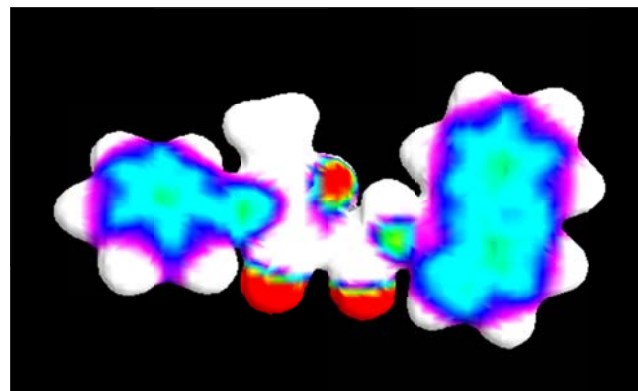


Fig. (4). Electron density distribution in the keto form of **1**.

to the molecule of **1** from crystallographic studies. The alignment on the pyrazolone system of both structures of **1** is presented in (Fig. 2). It can be seen that the position of the naphthyl group is different in the X-ray and computed structure, while the position of phenyl group is similar. Further conformational analysis studies may help to obtain a more accurate structure. HOMO and LUMO orbitals for **1** are shown in (Fig. 3), whereas the distribution of electron density for **1** is depicted in (Fig. 4). Naturally, the highest electron density occurs on both oxygen atoms, and on the amino nitrogen atom.

Boltzman Distribution Studies in Relation to Antibacterial Activity

The energy for both the keto and hydroxyl tautomers of **1** was calculated for isolated molecules (gas phase) and molecules in DMSO and water solutions. It was determined that in the gas phase the keto form is more stable with the stabilization energy of 15 kcal/mol whereas in DMSO solution the hydroxyl tautomer is favored with the stabilization energy of 5.58 kcal/mol. The population of the hydroxy form estimated using non-degenerate Boltzman distribution is less than 0.01% the crystalline form and about 99.99% in DMSO and water at 25 °C. The results of the calculations are in good agreement with the experimental data obtained from X-ray analysis and NMR and IR spectra. It can be hypothesized that antibacterial activity of **1** may be related to the greatest stability of its hydroxy form as it would ensure the formation of proper hydrogen bonds with bacterial enzymes.

IR Spectra

IR spectra were recorded without a solvent and in DMSO and also computed with the B3LYP DFT method. The ATR IR spectrum indicates an absence of a hydroxyl group thus suggesting that the molecule exists as a keto form in solid state which is supported by a strong band at 1712 cm^{-1} . Also, a single spike at 3449 cm^{-1} can contribute to a secondary amine (Fig. 5A).

In order to obtain a reliable spectrum of **1** in DMSO, the solvent was dried as described in the Materials and Methods. Next, the spectrum of dried DMSO was overlapped with the spectrum of **1** in dried DMSO (Fig. 5B). The DMSO spectrum (blue) exhibits no signals in the range of 3000 – 3600 cm^{-1} , which would indicate the presence of OH groups. Furthermore, this spectrum contains only signals which are characteristic for the dried DMSO. The spectrum of **1** recorded after deduction of DMSO (measured in the background) is the spectrum of **1** excluding those regions in which the solvent absorbs strongly.

A widened band of 3428 cm^{-1} in the spectrum of **1** in the dried DMSO represents a hydroxyl group. It is generally known that the hydroxyl group exhibits a characteristic absorption in the range 3000-3600 cm^{-1} [34, 35]. This corresponds to the stretching vibration band of the hydroxyl group. Furthermore, hydroxyl groups which do not undergo this association, exhibit a relatively narrow band of 3580-3670 cm^{-1} . This band is observed in the spectra of the diluted solutions of alcohols and phenols. The process of association may lead to the formation of a network of hydrogen bonds in

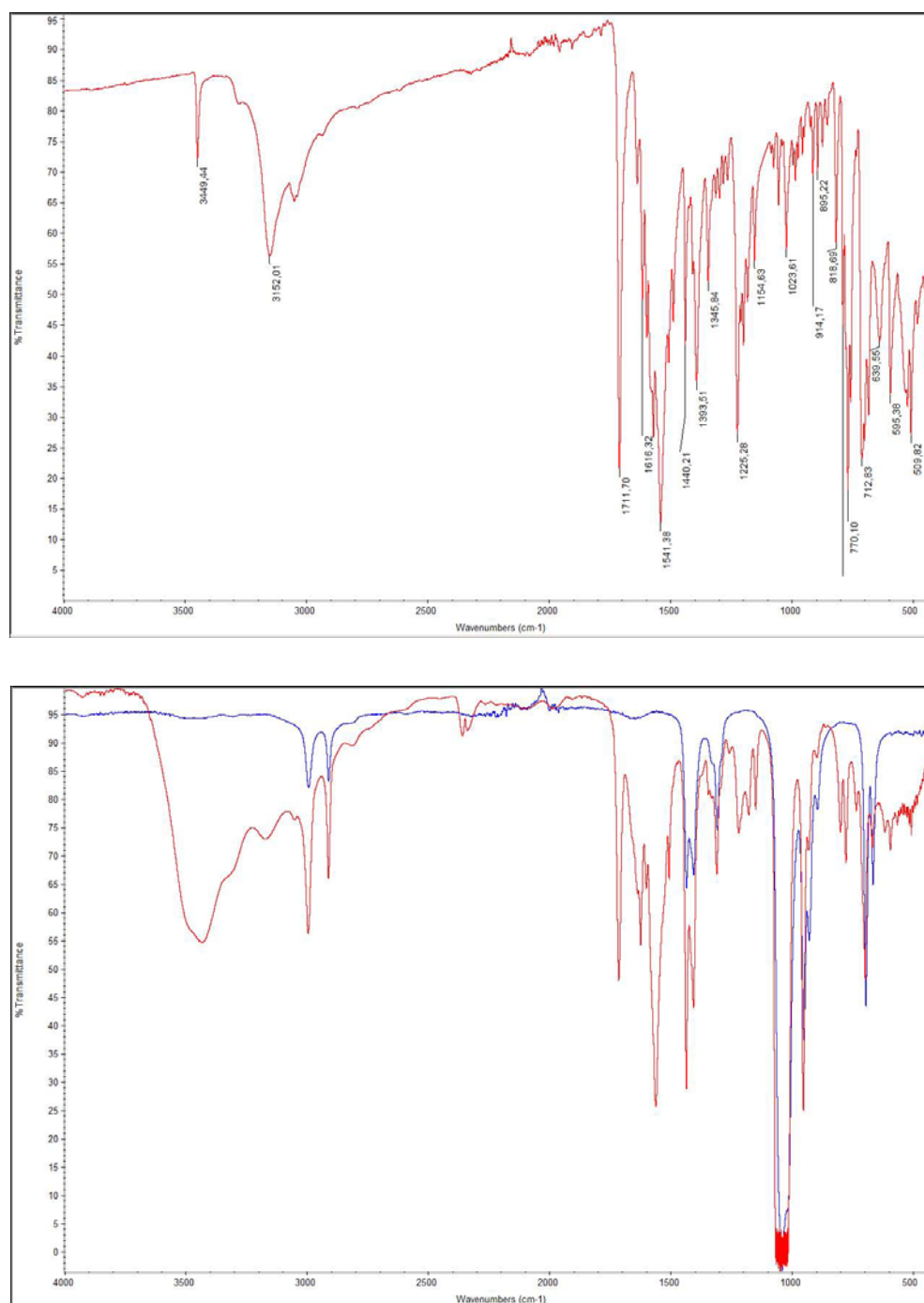


Fig. (5). A - ATR IR spectrum of **1**; B - IR spectrum of **1** in dried DMSO (red) overlapped with spectrum of dried DMSO (blue).

more concentrated solutions of compounds possessing hydroxyl groups. This phenomenon affects the shape and position of the absorption bands of the hydroxyl group stretching vibration through the formation of dimers and polymers resulting in the broad band in the range of 3200-3400 cm^{-1} . The observed value of hydroxyl group band for **1** indicates that the investigated compound may at least partially undergo association in the DMSO solution. It should also be pointed out that DMSO will bond extensively with molecule NH or OH groups, having impact upon the observed OH stretch. It can be thus seen from (Fig. 5B) that

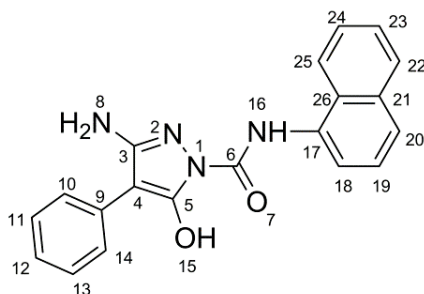
in DMSO solution the tautomeric equilibrium is shifted towards the form with the hydroxy group at position 5 which is confirmed by the computational data discussed above.

The IR data for the frequencies connected with the tautomerism of the investigated compounds are presented in (Table 2). It can be concluded that IR spectroscopy is a reliable method to investigate tautomerism in organic compounds. This confirms our earlier results [5, 36], and results by other authors obtained with IR [37] and Raman spectroscopy [38] approaches.

Table 2. Experimental and Computed IR Frequencies Involved in the Tautomerism of Compound 1

IR	N-H (cm ⁻¹)		C=O (cm ⁻¹)		OH (cm ⁻¹)	
	Exp.	Calc.	Exp.	Calc.	Exp.	Calc.
ATR	3449	3486	1711	1741	-	-
DMSO	-	-	-	-	3428	3340

Table 3. Experimental and Computed Chemical Shifts of 1 in DMSO



Atom	H			C		
	Exp.	Comp.		Exp.	Comp.	
		Keto	Hydroxy		Keto	Hydroxy
3	-	-	-	156.19	150.57	148.09
4	-	-	-	86.70	90.46	92.37
5	-	-	-	163.93	158.25	148.57
6	-	-	-	148.16	141.42	145.71
8	6.86	4.52	3.69	-	-	-
9	-	-	-	132.08	127.41	126.97
10, 14	7.66	7.85	7.77	127.21	120.66	120.38
11, 13	7.40	7.61	7.59	128.73	122.94	122.90
12	7.20	7.41	7.39	125.39	120.09	119.68
15	10.94	-	11.17	-	-	-
16	12.00	7.80	8.99	-	-	-
17	-	-	-	133.44	129.12	127.34
18	8.24	8.77	8.44	116.78	111.74	112.52
19	7.55	7.71	7.74	126.46	120.69	120.46
20	7.72	7.75	7.84	124.09	118.98	120.53
21	-	-	-	134.17	128.21	128.36
22	7.99	8.00	8.05	129.17	123.89	123.99
23	7.60	7.77	7.79	126.73	120.44	120.77
24	7.67	7.81	7.86	127.07	120.54	121.00
25	8.11	8.10	8.19	120.78	114.71	115.02
26	-	-	-	125.38	119.81	120.16

NMR Spectra

The experimental and computed NMR data of **1** is presented in (Table 3). All proton and carbon resonances were assigned by the combined application of standard 1D and 2D NMR techniques (^1H -decoupled ^{13}C NMR, COSY with gradient pulses, ^1H - ^{13}C multiplicity edited HSQC with gradient selection [39-44], ^1H - ^{13}C HMBC with gradient selection using low pass J-filter, Phase sensitive NOESY [45-46] and Phase sensitive ^1H - ^{15}N HSQC). Computed ^1H and ^{13}C chemical shifts for the keto and the hydroxyl tautomer cannot be

unambiguously related to experimental NMR spectrum. However, some values of calculated chemical shifts for the hydroxyl tautomer are close to the experimental values.

With resonances of exchangeable protons being not completely reliable we decided to investigate N-HSQC information which would reveal how many nitrogen atoms are protonated. Using short pulse sequence hsqcetgp, it was revealed that only two nitrogen atoms are connected directly to protons (Fig. 6) hence suggesting that only enol form might be present in solution. However taking into consideration the

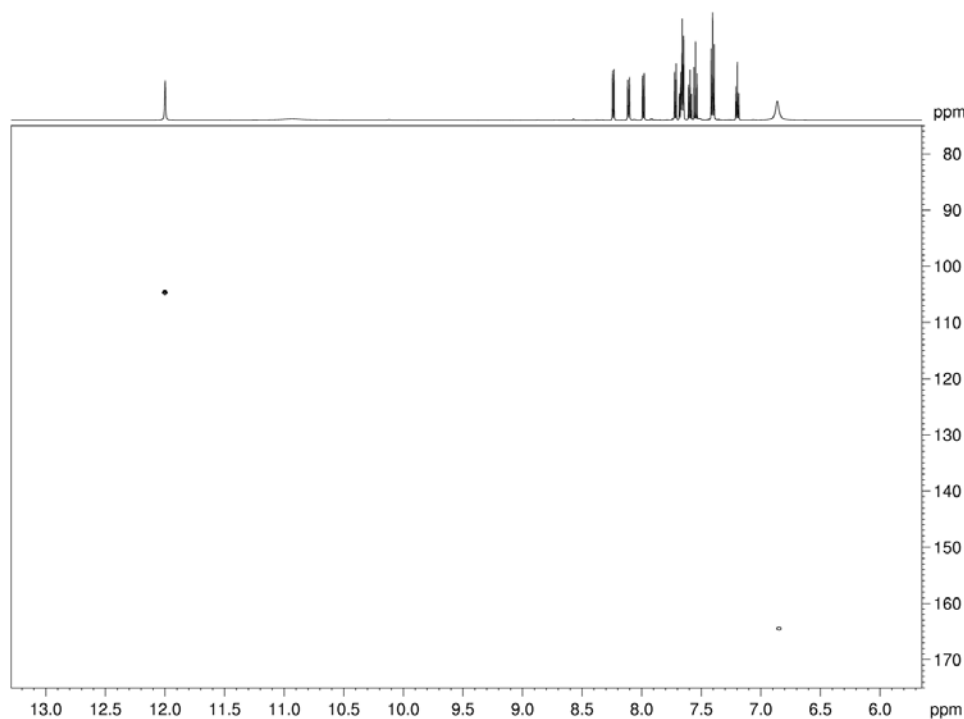


Fig. (6). N-H HSQC spectrum showing only two nitrogens with protons.

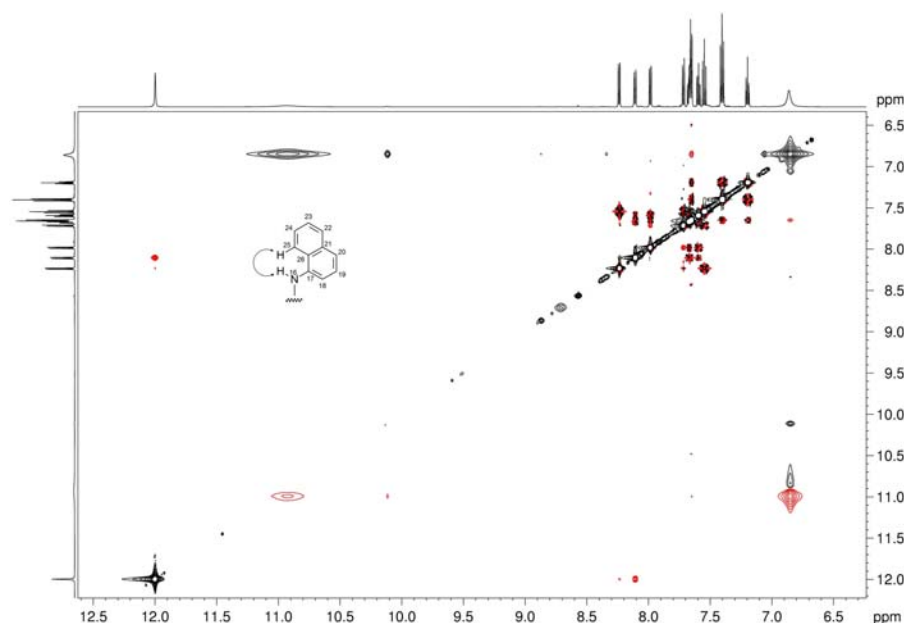


Fig. (7). NOESY spectrum indicating closeness of protons 25 and 16.

broadness of 10.94 ppm signal it is also possible that the keto form is also present but does not show the expected correlation despite using short pulse sequence. On the other hand this chemical shift is more likely to be that of enol rather than imine. Moreover, it can be inferred from the NOESY spectrum that naphthalene ring assumes position that places its 25 hydrogen close to hydrogen 16 (Fig. 7).

The tautomerism in similar systems was investigated by Holzer *et al.* [47] who determined that apart from chemical shift considerations and NOE effects the magnitude of the geminal 2*J* [pyrazole C-4,H3(5)] spin coupling constant permits the unambiguous differentiation between 1*H*-pyrazol-5-ol (OH) and 1,2-dihydro-3*H*-pyrazol-3-one (NH) forms. Performing such an experiment was not possible in case of **1** due to the lack of protons directly attached to the pyrazole ring and thus an impossibility of measuring relevant 2*J* C-H couplings. The NMR spectroscopy was also applied by Abood and Al-Shlhai [48] who concluded that the keto form is the preferred one for pyrazol-5-one and its derivatives in solutions, which contrasts our data. Enchev and Neykov [49] confirmed, however, by means of semiempirical calculations that in gas phase the keto tautomer is preferred which we also found for **1**.

CONCLUSION

In this study we find that the tautomer with the keto group in position 5 of *N*-(1-naphthyl)-3-amino-5-oxo-4-phenyl-1*H*-pyrazole-1-carboxamide with antibacterial is energetically privileged in the crystalline state, while in DMSO and water solution, the equilibrium is shifted towards the form with the hydroxyl group at this position. This finding is hypothesized to be related to antibacterial activity of the studied compound and is crucial for future molecular docking and structure-activity relationship studies.

CONFLICT OF INTEREST

The authors confirm that this article content has no conflict of interest.

ACKNOWLEDGEMENTS

The presented research was partially performed during the postdoctoral stay of Agnieszka A. Kaczor at the University of Eastern Finland, Kuopio, Finland, under a Marie Curie fellowship. Calculations were performed under a computational grant from the Interdisciplinary Center of Mathematical and Computational Modeling (ICM) in Warsaw, Poland, grant number G30-18 and under resources of CSC Finland. The paper was developed using equipment purchased under the project "The equipment of innovative laboratories doing research on new medicines used in the therapy of civilization and neoplastic diseases" within the Operational Programme Development of Eastern Poland 2007-2013, Priority Axis I Modern Economy, operations I.3 Innovation promotion

ABBREVIATIONS

CSGT = Continuous Set of Gauge Transformations

DFT = Density Functional Theory

FMO = Frontier Molecular Orbitals

HOMO = Highest Occupied Molecular Orbital

LUMO = Lowest Unoccupied Molecular Orbital

PCM = Polarizable Continuum Model

REFERENCES

- [1] Matosiuk, D.; Fidecka, S.; Antkiewicz-Michaluk, L.; Dybala, I.; Koziol, A. E. Synthesis and pharmacological activity of new carbonyl derivatives of 1-aryl-2-iminoimidazolidine. Part 1. Synthesis and pharmacological activity of chain derivatives of 1-aryl-2-iminoimidazolidine containing urea moiety. *Eur. J. Med. Chem.*, **2001**, *36*, 783-797.
- [2] Matosiuk, D.; Fidecka, S.; Antkiewicz-Michaluk, L.; Dybala, I.; Koziol, A. E. Synthesis and pharmacological activity of new carbonyl derivatives of 1-aryl-2-iminoimidazolidine. Part 3. Synthesis and pharmacological activity of 1-aryl-5,6(1*H*)dioxo-2,3-dihydroimidazo[1,2-*a*]imidazoles. *Eur. J. Med. Chem.*, **2002**, *37*, 845-853.
- [3] Matosiuk, D.; Fidecka, S.; Antkiewicz-Michaluk, L.; Lipkowski, J.; Dybala, I.; Koziol, A. E. Synthesis and pharmacological activity of new carbonyl derivatives of 1-aryl-2-iminoimidazolidine: Part 2. Synthesis and pharmacological activity of 1,6-diaryl-5,7(1*H*)dioxo-2,3-dihydroimidazo[1,2-*a*][1,3,5]triazines. *Eur. J. Med. Chem.*, **2002**, *37*, 761-772.
- [4] Sztanke, K.; Fidecka, S.; Kedzierska, E.; Karczmarzyk, Z.; Pihlaja, K.; Matosiuk, D. Antinociceptive activity of new imidazolidine carbonyl derivatives. Part 4. Synthesis and pharmacological activity of 8-aryl-3,4-dioxo-2*H*,8*H*-6,7-dihydroimidazo[2,1-*c*][1,2,4]triazines. *Eur. J. Med. Chem.*, **2005**, *40*, 127-134.
- [5] Kaczor, A. A.; Pitucha, M.; Karczmarzyk, Z.; Wysocki, W.; Rzymowska, J.; Matosiuk, D. Structural and molecular docking studies of 4-benzyl-3-[(1-methylpyrrol-2-yl)methyl]-4,5-dihydro-1*H*-1,2,4-triazol-5-one with anticancer activity. *Med. Chem.*, **2013**, *9*, 313-328.
- [6] Chu, C. K.; Cutler, S. J. Chemistry and antiviral activities of acyclonucleosides. *J. Heterocycl. Chem.*, **1986**, *23*, 289-319.
- [7] Rostom, S. A. F.; Shalaby, M. A.; El-Demellawy, M. A. Polysubstituted Pyrazoles, Part 5. Synthesis of new 1-(4-chlorophenyl)-4-hydroxy-1*H*-pyrazole-3-carboxylic acid hydrazide analogs and some derived ring systems. A novel class of potential antitumor and anti-HCV agents. *Eur. J. Med. Chem.*, **2003**, *38*, 959-974.
- [8] Singh, P.; Paul, K.; Holzer, W. Synthesis of Pyrazole-based Hybrid molecules: search for potent multidrug resistance modulators. *Bioorg. Med. Chem.*, **2006**, *14*, 5061-5071.
- [9] Chande, M. S.; Barve, P. A.; Suryanarayan, V. Synthesis and antimicrobial activity of novel spirocompounds with pyrazolone and pyrazolthione moiety. *J. Heterocycl. Chem.*, **2007**, *44*, 49-53.
- [10] Gok, S.; Demet, M. M.; Özdemir, A.; Turan-Zitouni, G. Evaluation of antidepressant-like effect of 2-pyrazoline derivatives. *Med. Chem. Res.*, **2010**, *19*, 94-101.
- [11] Rahimizadeh, M.; Pordel, M.; Bakavoli, M.; Rezaeian, S.; Sadeghian, A. Synthesis and antibacterial activity of some new derivatives of pyrazole. *World J. Microbiol. Biotechnol.*, **2010**, *26*, 317-321.
- [12] Khalilullah, H.; Khan, S.; Ahsan, M. J.; Ahmed, B. Synthesis and antihepatotoxic activity of 5-(2,3-dihydro-1,4-benzodioxane-6-yl)-3-substituted-phenyl-4,5-dihydro-1*H*-pyrazole derivatives. *Bioorg. Med. Chem. Lett.*, **2011**, *21*, 7251-7254.
- [13] Mor, S.; Mohil, R.; Kumar, D.; Ahuja, M. Synthesis and antimicrobial activities of some isoxazolyl thiazolyl pyrazoles. *Med. Chem. Res.*, **2011**, *21*, 3541-3548.
- [14] Thalassitis, A.; Katsori, A.M.; Dimas, K.; Hadjipavlou-Litina, D.J.; Pylaris, F.; Sakellariadis, N.; Litinas, K.E. Synthesis and biological evaluation of modified purine homo-N-nucleosides containing pyrazole or 2-pyrazoline moiety. *J. Enzyme Inhibit. Med. Chem.*, DOI:10.3109/14756366.2012.755623.
- [15] Helio, G.; Bonacorso, C.A.C. β -Alkoxyvinyl trifluoromethyl ketones as efficient precursors for the one-pot synthesis of bis-(4,5-dihydro-1*H*-pyrazol-1-yl)methanones and 1*H*-pyrazolyl-1-carbohydrazides. *ARKIVOC*, **2009**, *2*, 174-182.

- [16] Pitucha, M.; Kosikowska, U.; Mazur, L.; Malm, A. Synthesis, structure and antibacterial evaluation of some N-substituted 3-amino-5-hydroxy-4-phenyl-1H-pyrazole-1-carboxamides. *Med. Chem.*, **2011**, *7*, 697-703.
- [17] SADABS (Version 2004/1), Bruker AXS Inc., Madison, Wisconsin, USA, **2005** (Accessed March, 12, 2013).
- [18] Sheldrick, G. M. A short history of SHELX. *Acta Cryst.* **2008**, *A64*, 112-122.
- [19] Farrugia, L. J. WinGX suite for small-molecule single-crystal crystallography. *J. Appl. Cryst.*, **1999**, *32*, 837-838.
- [20] Armarego, W.L.F.; Chai, C.L.L. *Purification of Laboratory Chemicals*, 6th ed.; Elsevier: Oxford, **2009**.
- [21] Becke, A. Density-functional thermochemistry. III. the role of exact exchange. *J. Chem. Phys.*, **1993**, *98*, 5648-5652.
- [22] Lee; Yang; Parr development of the Colle-Salvetti correlation-energy formula into a functional of the electron density. *Phys. Rev. B Condens. Matter.*, **1988**, *37*, 785-789.
- [23] Frisch, M.J.; Trucks, G.W.; Schlegel, H.B.; Scuseria, G.E.; Robb, M.A.; Cheeseman, J.R.; Montgomery, J.A.; Vreven, T.; Kudin, K.N.; Burant, J.C.; Millam, J.M.; Iyengar, S.S.; Tomasi, J.; Barone, V.; Mennucci, B.; Cossi, M.; Scalmani, G.; Rega, N.; Petersson, G.A.; Nakatsuji, H.; Hada, M.; Ehara, M.; Toyota, K.; Fukuda, R.; Hasegawa, J.; Ishida, M.; Nakajima, T.; Honda, Y.; Kitao, O.; Nakai, H.; Klene, M.; Li, X.; Knox, J.E.; Hratchian, H.P.; Cross, J.B.; Bakken, V.; Adamo, C.; Jaramillo, J.; Gomperts, R.; Stratmann, R.E.; Yazyev, O.; Austin, A.J.; Cammi, R.; Pomelli, C.; Ochterski, J.W.; Ayala, P.Y.; Morokuma, K.; Voth, G.A.; Salvador, P.; Dannenberg, J.J.; Zakrzewski, V.G.; Dapprich, S.; Daniels, A.D.; Strain, M.C.; Farkas, O.; Malick, D.K.; Rabuck, A.D.; Raghavachari, K.; Foresman, J.B.; Ortiz, J.V.; Cui, Q.; Baboul, A.G.; Clifford, S.; Cioslowski, J.; Stefanov, B.B.; Liu, G.; Liashenko, A.; Piskorz, P.; Komaromi, I.; Martin, R.L.; Fox, D.J.; Keith, T.; Al-Laham, M.A.; Peng, C.Y.; Nanayakkara, A.; Challacombe, M.; Gill, P.M.W.; Johnson, B.; Chen, W.; Wong, M.W.; Gonzalez, C.; Pople, J.A. Gaussian 09, Gaussian Inc., **2009**, Wallingford CT.
- [24] Keith, T. A.; Bader, R. F. W. Calculation of magnetic response properties using atoms in molecules. *Chem. Phys. Lett.*, **1992**, *194*, 1-8.
- [25] Keith, T. A.; Bader, R. F. W. Calculation of magnetic response properties using a continuous set of gauge transformations. *Chem. Phys. Lett.*, **1993**, *210*, 223-231.
- [26] Cheeseman, J. R.; Trucks, G. W.; Keith, T. A.; Frisch, M. J. A comparison of models for calculating nuclear magnetic resonance shielding tensors. *J. Chem. Phys.*, **1996**, *104*, 5497-5509.
- [27] Miertus, S.; Tomasi, Approximate evaluations of the electrostatic free energy and internal energy changes in solution processes. *J. Chem. Phys.*, **1982**, *65*, 239-245.
- [28] The graphical program for working with quantum chemistry computations. <http://chemcraftprog.com> (Accessed March, 12, 2013).
- [29] The PyMOL Molecular Graphics System, Version 0.99, Schrödinger, LLC (Accessed March, 12, 2013).
- [30] Accelrys Software Inc., Discovery Studio Modeling Environment, Release 4.0, San Diego: Accelrys Software Inc. (Accessed March, 03, 2013).
- [31] Krieger, E.; Vriend, G. Models@Home: distributed computing in bioinformatics using a screensaver based approach. *Bioinformatics*, **2002**, *18*, 315-318.
- [32] Mercury - Crystal Structure Visualisation, Exploration and Analysis Made Easy. <http://www.ccdc.cam.ac.uk/support/documentation/#mercury> (Accessed March, 12, 2013).
- [33] Molecular modeling, graphics, and drug design program for Windows operating systems. <http://www.arguslab.com/arguslab.com/ArgusLab.html> (Accessed March, 11, 2013).
- [34] Silverstein, R.M.; Bassler, G.C.; Morrill, T.C. *Spectrometric Identification of Organic Compounds*, 5th ed; John Wiley & Sons: New York, **1991**.
- [35] Hesse, M.; Maier, H.; Zeeh, B. *Spectroscopic Methods in Organic Chemistry*, 2nd ed.; Georg-Thieme Verlag Stuttgart: New York, **2008**.
- [36] Pitucha, M.; Karczmarzyk, Z.; Wsocki, W.; Kaczor, A. A.; Matosiuk, D. Experimental and theoretical investigations on the keto-enol tautomerism of 4-substituted 3-[1-methylpyrrol-2-yl)methyl]-4,5-dihydro-1H-1,2,4-triazol-5-one derivatives. *J. Mol. Str.*, **2011**, *994*, 313-320.
- [37] Infantes L.; Foces-Foces C.; Claramunt R.M.; Lopez C.; Elguero J. Tautomerism of NH-pyrazolinones in the solid state: the case of 3(5)-ethoxycarbonyl-5(3)-hydroxypyrazole. *J. Mol. Struct.*, **1998**, *447*, 71-79.
- [38] Akama, Y.; Tong, A.; Matsumoto, N.; Ikeda, T.; Tanaka, S. Raman-spectroscopic study on keto-enol tautomers of 1-phenyl-3-methyl-4-benzoyl-5-pyrazolone. *Vibr. Spectr.*, **1996**, *13*, 113-115.
- [39] Palmer, A. G. III; Cavanagh, J.; Wright, P. E.; Rance, M. Sensitivity improvement in proton-detected 2-dimensional heteronuclear correlation NMR spectroscopy. *J. Magn. Reson.*, **1991**, *93*, 151-170.
- [40] Kay, L. E.; Keifer, P.; Saarinen, T. Pure absorption gradient enhanced heteronuclear single quantum correlation spectroscopy with improved sensitivity. *J. Am. Chem. Soc.*, **1992**, *114*, 10663-10665.
- [41] Schleucher, J.; Schwendinger, M.; Sattler, M.; Schmidt, P.; Schedletsky, O.; Glaser, S. J.; Sorensen, O. W.; Griesinger, C. A general enhancement scheme in heteronuclear multidimensional NMR employing pulsed field gradients. *J. Biomol. NMR.*, **1994**, *4*, 301-306.
- [42] Willker, W.; Leibfritz, D.; Kerssebaum, R.; Bermel, W. Gradient selection in inverse heteronuclear correlation spectroscopy. *Magn. Reson. Chem.*, **1993**, *31*, 287-292.
- [43] Zwaalen, C.; Legault, P.; Vincent, S. J. F.; Greenblatt, J.; Konrat, R.; Kay, L. E. Methods for measurement of intermolecular NOEs by multinuclear NMR spectroscopy: application to a bacteriophage λ N-peptide/boxB RNA complex. *J. Am. Chem. Soc.*, **1997**, *119*, 6711-6721.
- [44] Boyer, R. D.; Johnson, R.; Krishnamurthy, K. Compensation of refocusing inefficiency with synchronized inversion sweep (CRISIS) in multiplicity-edited HSQC. *J. Magn. Reson.*, **2003**, *165*, 253-259.
- [45] Jeener, J.; Meier, B. H.; Bachmann, P.; Ernst, R. R. Investigation of exchange processes by two-dimensional NMR spectroscopy. *J. Chem. Phys.*, **1979**, *71*, 4546-4553.
- [46] Wagner, R.; Berger, S. Gradient-selective NOESY- A fourfold reduction of the measurement time for the NOESY experiment. *J. Magn. Reson.*, **1996**, *123 A*, 119-121.
- [47] Holzer, W.; Kautsch, C.; Laggner, C.; Claramunt, R. M.; Pérez-Torralba, M.; Alkorta, I.; Elguero, J. On the tautomerism of pyrazolones: the geminal 2J[pyrazole C-4,H-3(5)] spin coupling constant as a diagnostic tool. *Tetrahedron*, **2004**, *60*, 6791-6805.
- [48] Abood, N. A.; Al-Shlhai, R. A. Theoretical study of molecular structure, IR and NMR spectra of pyrazolone and its derivatives. *J. Chem. Pharm. Res.*, **2012**, *4*, 1772-1781.
- [49] Enchev, V.; Neykov, G. D. A semiempirical and ab initio MO study of the tautomers of N-unsubstituted pyrazolones [hydroxy pyrazoles]. *Struct. Chem.*, **1992**, *3*, 231-238.